



Series solutions of nano boundary layer flows by means of the homotopy analysis method

Jun Cheng^a, Shijun Liao^{a,*}, R.N. Mohapatra^b, K. Vajravelu^b

^a School of Naval Architecture, Ocean and Civil Engineering, Shanghai Jiao Tong University, Shanghai 200030, China

^b Department of Mathematics, University of Central Florida, Orlando, FL 32816, USA

Received 4 September 2007

Available online 29 January 2008

Submitted by B. Straughan

Abstract

We present here a ‘similar’ solution for the nano boundary layer with nonlinear Navier boundary condition. Three types of flows are considered: (i) the flow past a wedge; (ii) the flow in a convergent channel; (iii) the flow driven by an exponentially-varying outer flows. The resulting differential equations are solved by the homotopy analysis method. Different from the perturbation methods, the present method is independent of small physical parameters so that it is applicable for not only weak but also strong nonlinear flow phenomena. Numerical results are compared with the available exact results to demonstrate the validity of the present solution. The effects of the slip length ℓ , the index parameters n and m on the velocity profile and the tangential stress are investigated and discussed.

© 2008 Elsevier Inc. All rights reserved.

Keywords: Boundary layer; Nano fluidics; Navier boundary condition; Homotopy analysis method

1. Introduction

In classical boundary layer theory, the *condition of no-slip* near solid walls is usually applied. The fluid velocity component is assumed to be zero relative to the solid boundary. This is not true for fluid flows at the micro and nano scale. Investigations show that the *condition of no-slip* is no longer valid. Instead, a certain degree of tangential slip must be allowed. To describe the phenomenon of slip, Navier [1] introduced a boundary condition which states the component of the fluid velocity tangential to the boundary walls is proportional to the tangential stress. Through the studies of fluids on the surface of various properties, later researchers [2–4] extended the linear Navier boundary condition to a nonlinear form

$$|u| = \ell \left(\left| \frac{\partial u}{\partial y} \right| \right)^n, \quad (1)$$

where $\ell > 0$ is the constant slip length and $n > 0$ is an arbitrary power parameter.

* Corresponding author.

E-mail address: sjliao@sjtu.edu.cn (S. Liao).

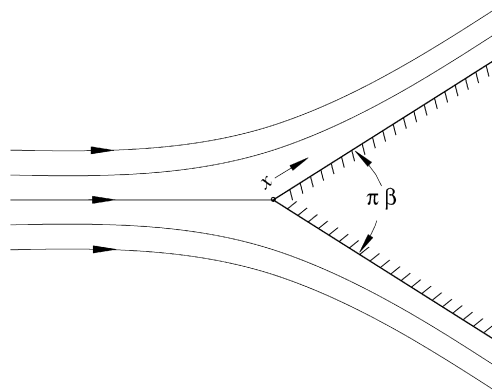


Fig. 1. Flow past a wedge.

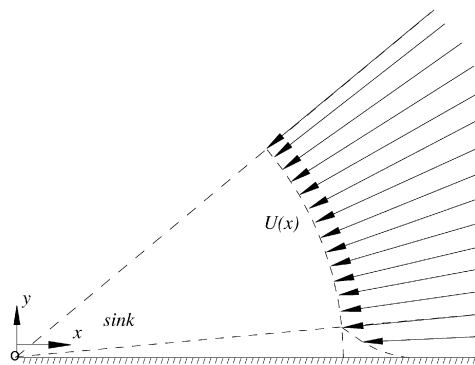


Fig. 2. Flow in a convergent channel.

In this paper, we shall restrict ourselves to the steady two-dimensional boundary layer with the differential equations

$$\frac{\partial u}{\partial x} + \frac{\partial v}{\partial y} = 0, \tag{2}$$

$$u \frac{\partial u}{\partial x} + v \frac{\partial u}{\partial y} = U \frac{dU}{dx} + \frac{\partial^2 u}{\partial y^2}, \tag{3}$$

subject to the boundary conditions

$$|u| = \ell \left(\left| \frac{\partial u}{\partial y} \right| \right)^n \quad \text{and} \quad v = 0 \quad \text{at} \quad y = 0, \tag{4}$$

$$u \equiv U(x) = ax^m \quad \text{as} \quad y \rightarrow \infty. \tag{5}$$

Here, x and y are the dimensionless Cartesian coordinates measured along the plate and normal to it which are scaled by a characteristic length of the body L and L/\sqrt{R} , respectively. u and v are the velocity components along the x and y axes which are scaled by the free-stream velocity U_∞ and U_∞/\sqrt{R} , respectively. U is a given external inviscid velocity field scaled by U_∞ . The constant $\ell > 0$ is the slip length scaled by $U_\infty^{1-n} L^n R^{-n/2}$. R denotes the Reynolds number; a , m and n are constants. The case $a > 0$ is of main interest when describing flows away from the origin, and $a < 0$ when the external stream flows towards the origin. The family of potential flows with $U(x) \sim x^m$ corresponds to flow past a wedge with angle $\pi\beta$, as shown in Fig. 1. It is known that the relationship between the wedge angle factor β and the exponent m is $\beta = 2m/(m + 1)$. Potential flows $U(x)$ proportional to $1/x$ correspond to the case of a two-dimensional sink or source depend on the sign of $U(x)$. When $a < 0$, it represents flow in a convergent channel with flat walls, as shown in Fig. 2 (for details see Schlichting [5]).

One of the most interesting problems arising out of finding a solution of boundary layer equation is the investigation of the conditions under which two solutions are similar. Using Lie symmetries analysis, Matthews and Hill [4,6] introduced the similarity transformation

$$\eta = x^{-\frac{n-1}{3n-2}} y \tag{6}$$

and the stream function $f(\eta)$ defined by

$$\frac{u}{U} = \frac{1}{a} f', \quad x^{\frac{2n-1}{3n-2}} \frac{v}{U} = \frac{1}{a} \left(\frac{n-1}{3n-2} \eta f' - \frac{2n-1}{3n-2} f \right), \tag{7}$$

provided $m = n/(3n - 2)$, where $n \neq 2/3$.

With these transformations, Eqs. (2) and (3) can be written as

$$f''' + \frac{2n-1}{3n-2} f f'' - \frac{n}{3n-2} (f'^2 - a^2) = 0, \tag{8}$$

where the prime denotes differentiation with respect to η . The boundary conditions depend on the value of n . For $n \neq 1/2$, the boundary conditions are

$$f = 0 \quad \text{and} \quad |f'| - \ell |f''|^n = 0 \quad \text{at} \quad \eta = 0, \tag{9}$$

$$f' \rightarrow a \quad \text{as} \quad \eta \rightarrow \infty. \tag{10}$$

For $n = 1/2$ the condition $f = 0$ will be replaced by

$$f'' \rightarrow 0 \quad \text{as} \quad \eta \rightarrow \infty. \tag{11}$$

As a matter of fact, these two kinds of boundary conditions correspond to two distinct physical phenomena. For $n = 1/2$ and $m = -1$, it corresponds to a two-dimensional sink provided $a < 0$. When $n \neq 1/2$, it corresponds to the flow past a wedge with angle $\pi\beta$. As is mentioned, the relationship between the wedge angle $\pi\beta$ and the exponent m is $\beta = 2m/(m + 1)$. In this analysis, since $m = n/(3n - 2)$ we have $\beta = n/(2n - 1)$. If we are concerned with boundary layers without back-flow or separation, we require $\beta > 0$ which implies $n > 1/2$. Particularly, $n = 1 \Rightarrow m = 1$ so that the wedge angle is π . This is the case of stagnation plane flow (Hiemenz flow) with the linear Navier boundary condition.

Now let us consider the special case for $n = 2/3$. Similar solutions exist when the potential flow $U(x) = a \exp(mx)$, which is a limiting case of $U(x) = ax^m$. Introducing the similarity transformation

$$\eta = y \exp\left(\frac{m}{2}x\right) \tag{12}$$

and the stream function $f(\eta)$ defined by

$$\frac{u}{U} = \frac{1}{a} f', \quad \exp\left(\frac{m}{2}x\right) \frac{v}{U} = -\frac{m}{2a} (\eta f' + f), \tag{13}$$

Matthews and Hill [4] obtained the ordinary differential equation

$$f''' + \frac{m}{2} f f'' - m(f'^2 - a^2) = 0 \tag{14}$$

and the boundary conditions (9) and (10).

A further simplification shows the parameter a can be removed from the governing equation and the boundary condition if η and ℓ are multiplied by $\sqrt{|a|}$ and $|a|^{\frac{3n}{2}-1}$, respectively; and f is multiplied by $1/\sqrt{a}$ for $a > 0$ and $-1/\sqrt{-a}$ for $a < 0$. Therefore, the differential equation for

(i) the flow away from the origin past a wedge is

$$f''' + \frac{2n-1}{3n-2} f f'' - \frac{n}{3n-2} (f'^2 - 1) = 0 \quad (a > 0); \tag{15}$$

(ii) the flow in a convergent channel is

$$f''' - f'^2 + 1 = 0 \quad (a < 0); \tag{16}$$

(iii) the special case when $n = 2/3$ and $U(x) = a \exp(mx)$ is

$$f''' + \frac{m}{2} f f'' - m(f'^2 - 1) = 0 \quad (a > 0), \tag{17}$$

$$f''' - \frac{m}{2} f f'' + m(f'^2 - 1) = 0 \quad (a < 0). \tag{18}$$

The boundary condition (10) becomes

$$f' \rightarrow 1 \quad \text{as } \eta \rightarrow \infty. \tag{19}$$

Generally speaking, the process of obtaining exact solutions of the nano boundary layer equations encounters considerable mathematical difficulties. Though it is possible to obtain the exact solutions in one or two particular cases (for example, the case of flows in a convergent channel), both the differential equations and the boundary conditions are nonlinear in most cases so that they can only be solved by numerical methods or series expansions. Matthews and Hill [4] have reported the numerical solution for the problem. In this paper, we obtain series solutions. As we know, the usual series method for nonlinear differential equations is the perturbation methods, in which one expands the solution with respect to a small parameter in power series so that the original differential equation is split into a system of simultaneous differential equations. However, perturbation methods are dependent upon small parameters so that they may lose validity for a comparatively large value of this parameter. To overcome the restriction, we shall apply a relatively new method, the homotopy analysis method [7–12], to examine the series solution of the nano boundary layer problem.

Proposed by Liao [7–12], the homotopy analysis method has been widely applied to many aspects of nonlinear problems, such as the viscous flows of non-Newtonian fluids [13–23], the KdV-type equations [24–28], nonlinear heat transfer [29–32], finance problems [33,34], Riemann problems related to nonlinear shallow water equations [35], projectile motion [36], Glauert-jet flow [37], nonlinear water waves [38], groundwater flows [39], Burgers–Huxley equation [40], time-dependent Emden–Fowler type equations [41], differential–difference equation [42], Laplace equation with Dirichlet and Neumann boundary conditions [43], thermal-hydraulic networks [44], boundary layer flows over a stretching surface with suction and injection [45], and so on. Especially, some new solutions of a few nonlinear equations are reported [46,47]: these new solutions have *never* been reported by all other previous analytic methods and even by numerical methods. This shows the great potential of the homotopy analysis method for strongly nonlinear problems in science and engineering. Different from perturbation techniques, this method is independent of any small parameters. Besides, unlike other analytic techniques, it provides us a simple way to ensure the convergence of series solution of a nonlinear problem. Therefore, it is particularly suitable for strongly nonlinear problems.

Here in this problem, the situation is different from other problems. The nonlinear Navier boundary condition contains the power parameter n . Suppose we constructed the homotopy *zero-order deformation equations* of the nonlinear Navier boundary condition as usual. Different values of n would consequently lead to totally different *high-order deformation equations*. Without loss of generality, we shall therefore use a trick in which a new boundary condition, $f'(0) = \alpha$, is substituted for the nonlinear Navier boundary condition. In the next section, we shall present the homotopy analysis method.

2. The homotopy analysis method

Here we have three kinds of ‘similar’ equations for the boundary layer equations (2) to (5). From the point of view of the boundary conditions, the case (i) is a more complicated than the other two cases because the case (i) contains the boundary condition (9) with an arbitrary power parameter n . To illustrate the homotopy analysis method clearly and representatively, we shall take the case (i) with Eqs. (15), (9) and (19) as example.

Based on the boundary conditions (9) and (19), it is reasonable to assume *the solution expression* to be

$$f(\eta) = \sum_{n=1, m=0}^{\infty} c_{m,n} \eta^m \exp(-n\eta). \tag{20}$$

Let us define a (jointly continuous) map $F(\eta; q) \mapsto f(\eta)$, where the embedding parameter is $q \in [0, 1]$ such that, as q increases from 0 to 1, $F(\eta; q)$ varies from an initial guess to the exact solution $f(\eta)$. To ensure this, we construct *the zero-order deformation equation* of the governing equation

$$(1 - q)\mathcal{L}[F(\eta; q) - f_0(\eta)] = \hbar H(\eta)q\mathcal{N}[F(\eta; q)]. \tag{21}$$

Let us substitute a new boundary condition, $f'(0) = \alpha$, for the original nonlinear Navier boundary condition. Thus the zero-order deformation equations of the boundary conditions (9) and (19) can be written as

$$F(0; q) = 0 \quad \text{and} \quad \frac{\partial F}{\partial \eta}(0; q) = \alpha \quad \text{at} \quad \eta = 0, \tag{22}$$

$$\frac{\partial F}{\partial \eta}(\eta; q) \rightarrow 1 \quad \text{as} \quad \eta \rightarrow \infty. \tag{23}$$

In (21), $\hbar \neq 0$ is an auxiliary parameter, $H(\eta) \neq 0$ is an auxiliary function of η , \mathcal{L} is the auxiliary linear operator defined by

$$\mathcal{L} = \frac{\partial^3}{\partial \eta^3} + \frac{\partial^2}{\partial \eta^2}, \tag{24}$$

and the operator $\mathcal{N}[F(\eta; q)]$ is defined from the differential equation (15) as

$$\mathcal{N}[F(\eta; q)] = \frac{\partial^3 F}{\partial \eta^3} + \frac{2n-1}{3n-2}F \frac{\partial^2 F}{\partial \eta^2} - \frac{n}{3n-2} \left[\left(\frac{\partial F}{\partial \eta} \right)^2 - 1 \right]. \tag{25}$$

When $q = 0$, the zero-order deformation equations (21) to (23) give rise to

$$F(\eta; 0) = f_0(\eta). \tag{26}$$

When $q = 1$, they become

$$F(\eta; 1) = f(\eta). \tag{27}$$

$f_0(\eta)$ is an initial guess which should satisfy the boundary conditions

$$f_0(0) = 0, \quad f_0'(\eta) = \alpha, \quad f_0'(\infty) = 1. \tag{28}$$

For example, we can assume

$$f_0(\eta) = \alpha - 1 + \eta - (\alpha - 1)\exp(-\eta) \tag{29}$$

as our initial guess. Hence it is seen that $f_0(\eta)$ and $f(\eta)$ are homotopic.

Expanding $F(\eta; q)$ in Maclaurin series with respect to the embedding parameter q , we obtain

$$F(\eta; q) = f_0(\eta) + \sum_{n=1}^{\infty} f_n(\eta)q^n, \tag{30}$$

where

$$f_n(\eta) = \frac{1}{n!} \frac{\partial^n}{\partial q^n} F(\eta; 0). \tag{31}$$

Assuming that above series is convergent for $q = 1$, we get

$$f(\eta) = f_0(\eta) + \sum_{n=1}^{\infty} f_n(\eta). \tag{32}$$

Differentiating the zero-order deformation equations (21) to (23) m times with respect to q , then setting $q = 0$, and finally dividing by $m!$, we obtain the high-order deformation equations ($m \geq 1$):

$$\mathcal{L}(f_m - \chi_m f_{m-1}) = \hbar H R_m, \tag{33}$$

$$f_m = 0 \quad \text{and} \quad f_m' = 0 \quad \text{at} \quad \eta = 0, \tag{34}$$

$$f_m' \rightarrow 0 \quad \text{as} \quad \eta \rightarrow \infty, \tag{35}$$

where

$$\chi_m = \begin{cases} 0, & m = 1, \\ 1, & m > 1, \end{cases} \tag{36}$$

and

$$R_m = f'''_{m-1} + \frac{2n-1}{3n-2} \sum_{i=0}^{m-1} f_i f''_{m-1-i} - \frac{n}{3n-2} \left(\sum_{i=0}^{m-1} f'_i f'_{m-1-i} - 1 + \chi_m \right). \tag{37}$$

For simplicity, assume $H = 1$; hence the solution of (33) can be expressed in the form

$$f_m = \chi_m f_{m-1} + \hbar \mathcal{L}^{-1} R_m + C_0 + C_1 \eta + C_2 \exp(-\eta), \tag{38}$$

where C_0, C_1, C_2 are determined by the substitution of (38) into (34) and (35).

It is known that the m th order solution $f''_m(\eta)$ must include the parameters \hbar and α . Assuming that the integer j is large enough to ensure convergence, from the series (32), we obtain

$$f''(0) \approx \sum_{i=0}^j f''_i(0) = s(\alpha, \hbar), \tag{39}$$

where s is a function of α and \hbar . Suppose the value of \hbar is chosen properly so that the solution series are convergent. We can solve α from the nonlinear Navier boundary condition

$$|\alpha| = \ell |s(\alpha, \hbar)|^n. \tag{40}$$

It is an algebraic equation. It is worth mentioning that (40) may have more than one real solution. However, not all of them are meaningful physically. For example, in the case of flow (away from the origin) past a wedge, the tangential velocity at the wall $\alpha \geq 0$ is required so that we should eliminate those values of $\alpha < 0$.

3. Result and discussion

In the previous section we have the assumption that \hbar is to be properly chosen so that the solution series are convergent. But how can we choose such a proper \hbar ? Commonly, we do this by means of the so-called \hbar -curve, in which we look upon the parameter α as an independent variable and $s(\alpha, \hbar)$ as its function. Let us take the case of the flow past a wedge governed by the differential equation (15), as shown in Fig. 3. It is known that α is the dimensionless tangential velocity on the wall. Thus, it should hold $\alpha \geq 0$. Within the area $0 \leq \alpha \leq 1$, it is seen that there exists an almost overlapping area of $s(\alpha, \hbar)$ for different values of \hbar , such as $\hbar = -0.01, \hbar = -0.03, \hbar = -0.05$. The larger \hbar is in magnitude, the more quickly the series solution converges. But too large \hbar in magnitude may lead to the divergence of the series solution. From Fig. 3, we can see that $-0.05 \leq \hbar < 0$ is the valid region of \hbar . As long as the series solution converges, it must be one of the solutions of the problem, as is proved by Liao [8].

In fact, there exists an effective and easy-to-use method to obtain the high-order approximation. That is the homotopy Padé method. It is found that the $[k, k]$ homotopy Padé approximants not only can accelerate the convergence of the series solution but also exclude the auxiliary parameter \hbar from it. The possible reason is that the Padé technique plays the role of a *filter* which filters out the most slowly decaying factors so as to accelerate the *transient process* and makes it stable. To show its advantages, we compare the different orders of homotopy Padé approximants with numerical results for differential equations (15) and (16) in Tables 1 and 2, respectively. As we know $f''(0)$ is related to the tangential stress. It can be seen the $[k, k]$ homotopy Padé approximants of $f''(0)$ agree well with the numerical results.

For the flow past a wedge which corresponds to the differential equation (15), the variation of $f''(0)$ with both the slip length ℓ and the wedge angle factor $\beta = n/(2n - 1)$ is shown in Fig. 4. The $[15, 15]$ homotopy Padé approximant and the numerical result agree well with each other. It is found that when ℓ approaches zero, $f''(0)$ increases with an increasing wedge angle; when ℓ is near or above one, $f''(0)$ decreases as the wedge angle increases.

The profiles for the x and y components of the velocity in the case of the flow past a wedge, when $n = 2$ corresponding to a wedge angle of $\frac{2}{3}\pi$, are illustrated in Figs. 5 and 6. The 35th-order homotopy approximation for $\hbar = -0.05$ and the numerical result are compared. For fixed n the velocity components increase in magnitude as the slip length increases.

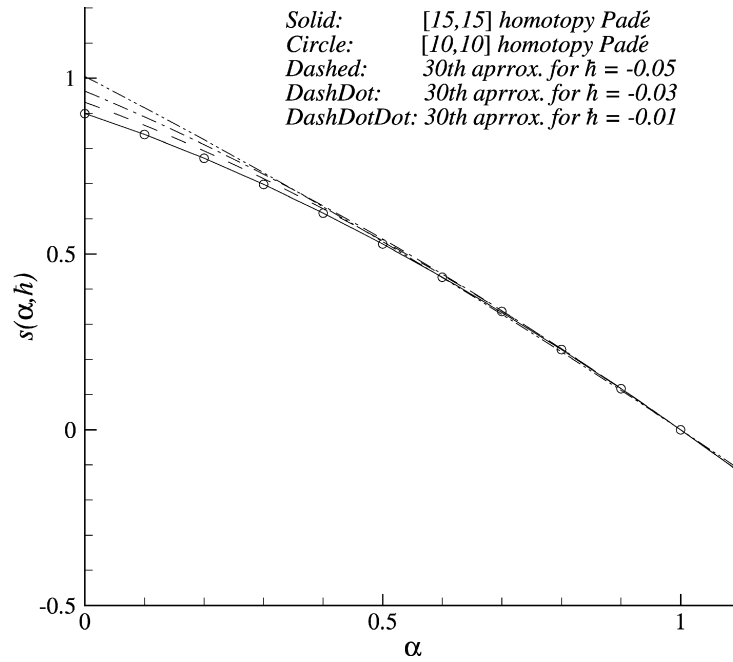


Fig. 3. The \hbar -curves of $s(\alpha, \hbar)$ for the differential equation (15). Solid: the [15, 15] homotopy Padé approximant for $s(\alpha, \hbar)$; circle: the [10, 10] homotopy Padé approximant for $s(\alpha, \hbar)$; dashed: the 30th-order homotopy approximation of $s(\alpha, -0.05)$; dashdot: the 30th-order homotopy approximation of $s(\alpha, -0.03)$; dashdotdot: the 30th-order homotopy approximation of $s(\alpha, -0.01)$.

Table 1

The $[k, k]$ homotopy Padé approximant of $f''(0)$ for the case of the flow past a wedge, where $n = 2$ and $\ell = 0, 0.1, 1$ and 10

$[k, k]$	$\ell = 0$	$\ell = 0.1$	$\ell = 1$	$\ell = 10$
[13, 13]	0.8994	0.8565	0.6243	0.2750
[14, 14]	0.8995	0.8566	0.6244	0.2750
[15, 15]	0.8996	0.8567	0.6246	0.2750
[16, 16]	0.8997	0.8567	0.6247	0.2750
[17, 17]	0.8997	0.8567	0.6247	0.2750
[18, 18]	0.8997	0.8567	0.6247	0.2750
Numerical	0.8997	0.8567	0.6247	0.2750

Table 2

The $[k, k]$ homotopy Padé approximant of $f''(0)$ for the case of the flow in a convergent channel, where $n = 1/2$ and $\ell = 0, 0.1, 1$ and 10

$[k, k]$	$\ell = 0$	$\ell = 0.1$	$\ell = 1$	$\ell = 10$
[13, 13]	1.1547	1.0620	0.4444	0.03788
[14, 14]	1.1547	1.0620	0.4444	0.03788
[15, 15]	1.1547	1.0620	0.4444	0.03788
[16, 16]	1.1547	1.0620	0.4444	0.03788
[17, 17]	1.1547	1.0620	0.4444	0.03788
[18, 18]	1.1547	1.0620	0.4444	0.03788
Exact	1.1547	1.0621	0.4444	0.03788

For the flow in a convergent channel, there exists an exact solution

$$f'(\eta) = 3 \tanh^2[\eta/\sqrt{2} + \tanh^{-1}(\lambda)] - 2, \tag{41}$$

where λ is the largest positive root of

$$9\lambda^4 + 3\sqrt{2}\ell^2\lambda^3 - 12\lambda^2 - 3\sqrt{2}\ell^2\lambda + 4 = 0. \tag{42}$$

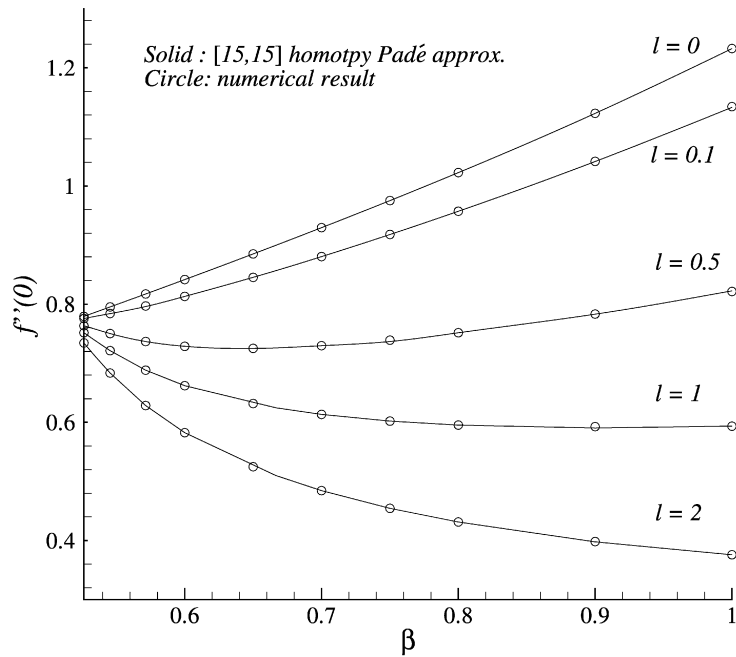


Fig. 4. The variation of $f''(0)$ with the wedge angle factor β in the case of the flow past a wedge. Solid: [15, 15] homotopy Padé approximant; circle: numerical result.

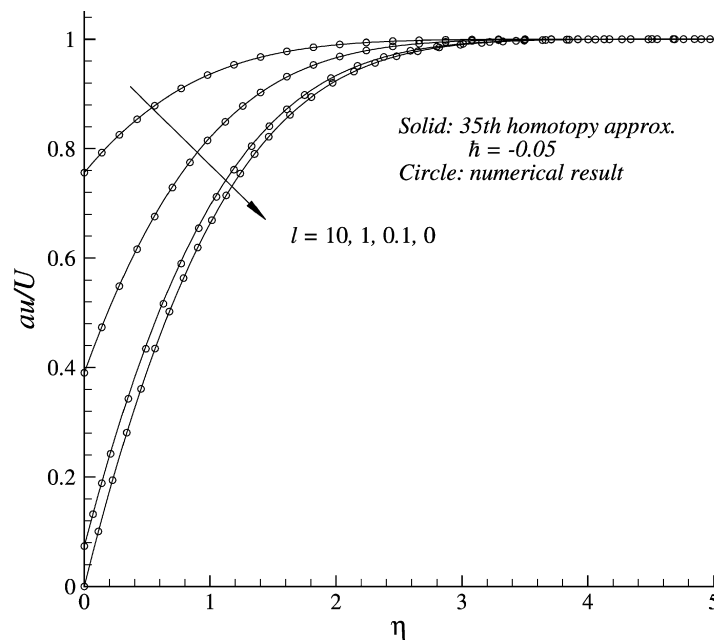


Fig. 5. Dimensionless velocity component u for $n = 2$ and $\ell = 0, 0.1, 1, 10$. Solid: 35th-order homotopy approximation when $\hbar = -1/20$; circle: numerical result.

In fact, the substitution of any positive root of (42) into (41) can satisfy the original differential equation (16) and its corresponding boundary conditions, but the smaller positive values of λ would lead to contradiction with our assumption of a two-dimensional sink.

By means of the homotopy analysis method, we can obtain the high-order series solution for (16). Since the boundary conditions are different in this case, it is necessary to change the initial guess, the linear operator, the auxiliary parameter \hbar and the auxiliary function $H(\eta)$, etc. For example, we introduce the new boundary condition $f''(0) = \alpha$ and assume

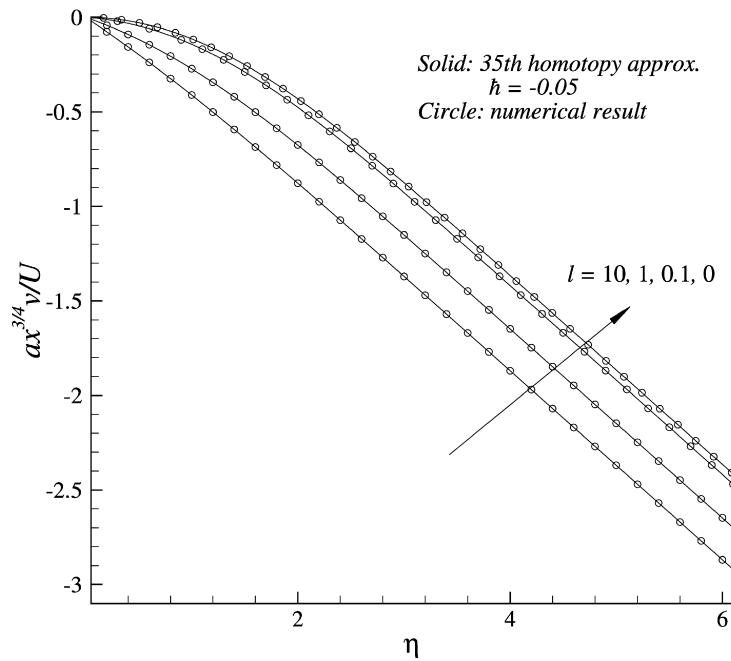


Fig. 6. Dimensionless velocity component v for $n = 2$ and $\ell = 0, 0.1, 1, 10$. Solid: 35th-order homotopy approximation when $\hbar = -1/20$; circle: numerical result.

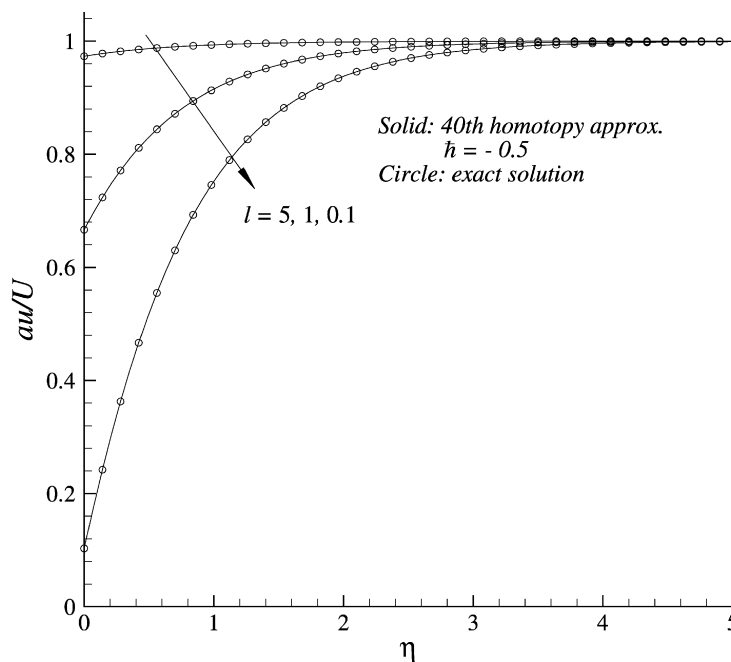


Fig. 7. Dimensionless velocity component u for $n = 1/2$ and $\ell = 0.1, 1, 5$. Solid: 40th-order homotopy approximation when $\hbar = -1/2$; circle: exact solution.

$$f_0'(\eta) = -\alpha \exp(-\eta) + 1, \quad \mathcal{L} = \frac{\partial^2}{\partial \eta^2} - 1, \quad H(\eta) = \exp(-\eta). \quad (43)$$

The valid region of \hbar is found to be $-0.8 < \hbar < 0$. Likewise, it is found that there may exist two solutions for α . We only retain the solution corresponding to the value of α which leads to $f'(0) > 0$. The x and y components of the velocity for $n = 1/2$ are shown in Figs. 7 and 8. The 40th-order homotopy approximation for $\hbar = -0.5$ and the numerical result are compared. When the slip length ℓ increases, the rate of change of the tangential velocity through the boundary layer decreases. However, there is little effect on the normal velocity component through out the boundary layer.

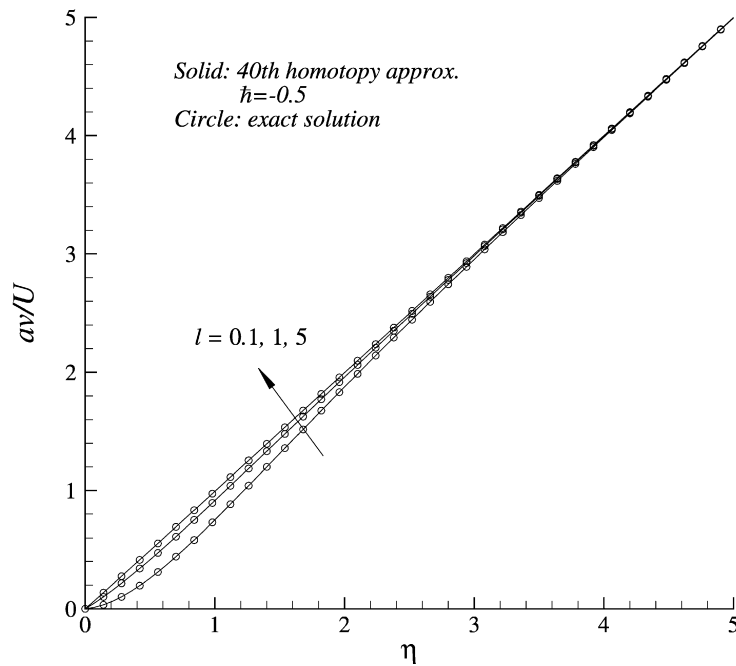


Fig. 8. Dimensionless velocity component v for $n = 1/2$ and $\ell = 0.1, 1, 5$. Solid: 40th-order homotopy approximation when $\hbar = -1/2$; circle: exact solution.

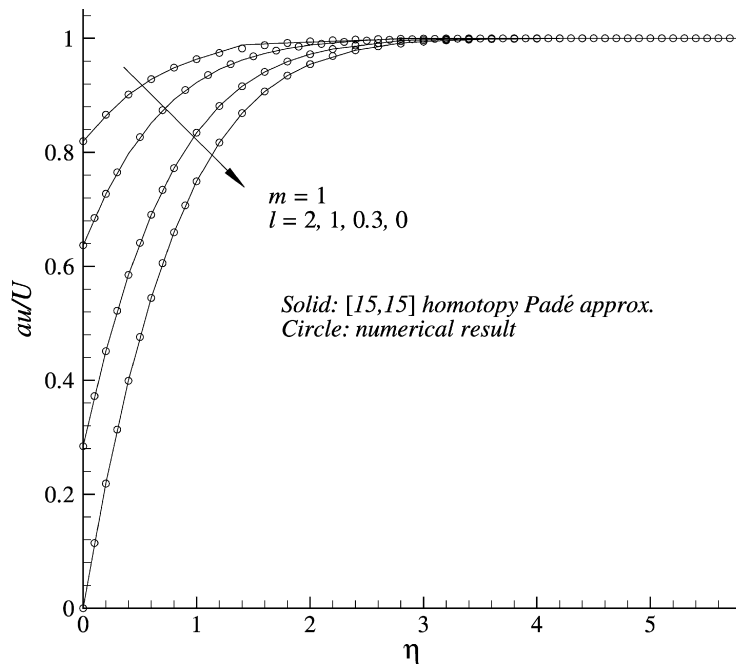


Fig. 9. Dimensionless velocity component u for $n = 2/3$, $m = 1$ and $\ell = 0, 0.3, 1, 2$. Solid: $[15, 15]$ homotopy Padé approximant; circle: numerical result.

For the case where $n = 2/3$ which corresponds to the potential flow with $U(x) = a \exp(mx)$, the homotopy analysis method, the initial guess $f_0(\eta)$, the linear operator \mathcal{L} and the auxiliary function $H(\eta)$ are the same as those we use in Section 2. Also we use the homotopy Padé method. Thus the auxiliary parameter \hbar can be eliminated from our approximations. Here we consider the case of $a > 0$. The $[15, 15]$ homotopy Padé approximant of the tangential velocity profile is compared with the numerical result, as shown in Figs. 9 and 10. It is found that for fixed m the tangential velocity increases as the slip length increases, and for fixed ℓ the tangential velocity increases as m increases.

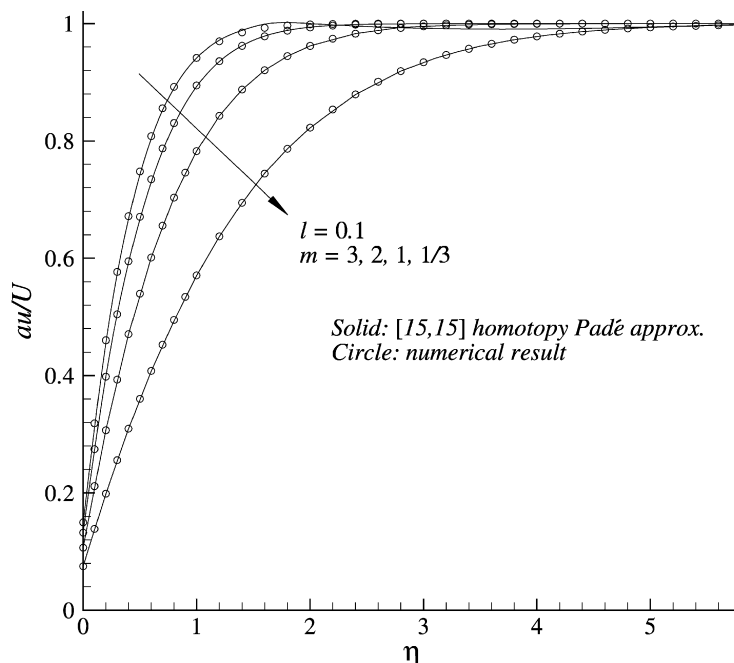


Fig. 10. Dimensionless velocity component u for $n = 2/3$, $\ell = 0.1$ and $m = 1/3, 1, 2, 3$. Solid: $[15, 15]$ homotopy Padé approximant; circle: numerical result.

4. Conclusion

The homotopy analysis method is applied to the nano boundary layer with nonlinear Navier boundary condition. Through the similarity transformation, we obtained series solutions for three different flow phenomena:

- (i) the flow past a wedge;
- (ii) the flow in a convergent channel;
- (iii) the flow driven by an exponentially-varying outer flow.

We compare the higher-order homotopy approximation results and the $[k, k]$ homotopy Padé approximant results with the numerical results of Matthews and Hill [4]. It is found that the present approximation agrees well with the numerical one. The effects of both ℓ and n on the velocity profile and the tangential stress are discussed. For the flow past a wedge, when ℓ approaches zero, $f''(0)$ increases as the wedge angle increases; however, when ℓ is near or above one, $f''(0)$ decreases. For the flow in a convergent channel, as ℓ increases, the rate of change of the tangential velocity decreases. For the flow driven by an exponentially-varying outer flow, for fixed m , the tangential velocity increases as ℓ increases, and for fixed ℓ , the tangential velocity increases as m increases.

Acknowledgments

The authors' thanks are due to the referee for the valuable comments for the improvement of the paper. This work is partly supported by the National Natural Science Foundation of China (Approve No. 10572095) and partly supported by the program for Changjiang scholars and innovative research team in university (Approve No. IRT0525).

References

- [1] C.L.M.H. Navier, Mémoire sur les lois du mouvement des fluides, Mém. Acad. Roy. Sci. Inst. France 6 (1823) 389–440.
- [2] Y.D. Shikhmurzaev, The moving contact line on a smooth solid surface, Int. J. Multiphase Flow 19 (1993) 589–610.
- [3] C.H. Choi, J.A. Westin, K.S. Breuer, To slip or not to slipwater flows in hydrophilic and hydrophobic microchannels, in: Proceedings of IMECE 2002, New Orleans, LA, Paper No. 2002-33707.
- [4] M.T. Matthews, J.M. Hill, Nano boundary layer equation with nonlinear Navier boundary condition, J. Math. Anal. Appl. 333 (2007) 381–400.
- [5] H. Schlichting, Boundary Layer Theory, McGraw–Hill, New York, 1979.

- [6] M.T. Matthews, J.M. Hill, A note on the boundary layer equations with linear slip boundary layer condition, *Appl. Math. Lett.* (2007), doi:10.1016/j.aml.2007.09.002, in press.
- [7] S.J. Liao, The proposed homotopy analysis technique for the solution of nonlinear problems, PhD thesis, Shanghai Jiao Tong University, 1992.
- [8] S.J. Liao, *Beyond Perturbation: Introduction to the Homotopy Analysis Method*, Chapman & Hall/CRC Press, Boca Raton, 2003.
- [9] S.J. Liao, An explicit, totally analytic approximation of Blasius viscous flow problems, *Internat. J. Non-Linear Mech.* 34 (4) (1999) 759–778.
- [10] S.J. Liao, On the homotopy analysis method for nonlinear problems, *Appl. Math. Comput.* 147 (2004) 499–513.
- [11] S.J. Liao, Y. Tan, A general approach to obtain series solutions of nonlinear differential equations, *Stud. Appl. Math.* 119 (2007) 297–355.
- [12] S.J. Liao, Beyond perturbation: Review on the basic ideas of the homotopy analysis method and its applications, *Adv. Mech.* 38 (1) (2008) 1–34 (in Chinese).
- [13] T. Hayat, T. Javed, M. Sajid, Analytic solution for rotating flow and heat transfer analysis of a third-grade fluid, *Acta Mech.* 191 (2007) 219–229.
- [14] T. Hayat, M. Khan, M. Sajid, S. Asghar, Rotating flow of a third grade fluid in a porous space with hall current, *Nonlinear Dynam.* 49 (2007) 83–91.
- [15] T. Hayat, M. Sajid, On analytic solution for thin film flow of a fourth grade fluid down a vertical cylinder, *Phys. Lett. A* 361 (2007) 316–322.
- [16] T. Hayat, M. Sajid, Analytic solution for axisymmetric flow and heat transfer of a second grade fluid past a stretching sheet, *Int. J. Heat Mass Transfer* 50 (2007) 75–84.
- [17] T. Hayat, Z. Abbas, M. Sajid, S. Asghar, The influence of thermal radiation on MHD flow of a second grade fluid, *Int. J. Heat Mass Transfer* 50 (2007) 931–941.
- [18] T. Hayat, M. Sajid, Homotopy analysis of MHD boundary layer flow of an upper-convected Maxwell fluid, *Internat. J. Engrg. Sci.* 45 (2007) 393–401.
- [19] T. Hayat, N. Ahmed, M. Sajid, S. Asghar, On the MHD flow of a second grade fluid in a porous channel, *Comput. Math. Appl.* 54 (2007) 407–414.
- [20] T. Hayat, M. Khan, M. Ayub, The effect of the slip condition on flows of an Oldroyd 6-constant fluid, *J. Comput. Appl.* 202 (2007) 402–413.
- [21] M. Sajid, A.M. Siddiqui, T. Hayat, Wire coating analysis using MHD Oldroyd 8-constant fluid, *Int. J. Engrg. Sci.* 45 (2007) 381–392.
- [22] M. Sajid, T. Hayat, S. Asghar, Non-similar analytic solution for MHD flow and heat transfer in a third-order fluid over a stretching sheet, *Int. J. Heat Mass Transfer* 50 (2007) 1723–1736.
- [23] M. Sajid, T. Hayat, S. Asghar, Non-similar solution for the axisymmetric flow of a third-grade fluid over radially stretching sheet, *Acta Mech.* 189 (2007) 193–205.
- [24] S. Abbasbandy, Soliton solutions for the 5th-order KdV equation with the homotopy analysis method, *Nonlinear Dynam.* 51 (2008) 83–87.
- [25] S. Abbasbandy, The application of the homotopy analysis method to solve a generalized Hirota–Satsuma coupled KdV equation, *Phys. Lett. A* 361 (2007) 478–483.
- [26] Y.P. Liu, Z.B. Li, The homotopy analysis method for approximating the solution of the modified Korteweg–de Vries equation, *Chaos Solitons Fractals*, in press.
- [27] L. Zou, Z. Zong, Z. Wang, L. He, Solving the discrete KdV equation with homotopy analysis method, *Phys. Lett. A* 370 (2007) 287–294.
- [28] L. Song, H.Q. Zhang, Application of homotopy analysis method to fractional KdV–Burgers–Kuramoto equation, *Phys. Lett. A* 367 (2007) 88–94.
- [29] S. Abbasbandy, The application of the homotopy analysis method to nonlinear equations arising in heat transfer, *Phys. Lett. A* 360 (2006) 109–113.
- [30] S. Abbasbandy, Homotopy analysis method for heat radiation equations, *Int. Commun. Heat Mass Transfer* 34 (2007) 380–387.
- [31] M. Sajid, T. Hayat, S. Asghar, Comparison between the HAM and HPM solutions of tin film flows of non-Newtonian fluids on a moving belt, *Nonlinear Dynam.* 50 (2007) 27–35.
- [32] M. Sajid, T. Hayat, Comparison of HAM and HPM methods for nonlinear heat conduction and convection equations, *Nonlinear Anal. Real World Appl.*, in press.
- [33] S.P. Zhu, An exact and explicit solution for the valuation of American put options, *Quant. Finance* 6 (2006) 229–242.
- [34] S.P. Zhu, A closed-form analytical solution for the valuation of convertible bonds with constant dividend yield, *ANZIAM J.* 47 (2006) 477–494.
- [35] Y. Wu, K.F. Cheung, Explicit solution to the exact Riemann problems and application in nonlinear shallow water equations, *Int. J. Numer. Methods Fluids*, in press.
- [36] M. Yamashita, K. Yabushita, K. Tsuboi, An analytic solution of projectile motion with the quadratic resistance law using the homotopy analysis method, *J. Phys. A* 40 (2007) 8403–8416.
- [37] Y. Bouremel, Explicit series solution for the Glauert–jet problem by means of the homotopy analysis method, *Commun. Nonlinear Sci. Numer. Simul.* 12 (5) (2007) 714–724.
- [38] L. Tao, H. Song, S. Chakrabarti, Nonlinear progressive waves in water of finite depth—an analytic approximation, *Clastal Engrg.* 54 (2007) 825–834.
- [39] H. Song, L. Tao, Homotopy analysis of 1D unsteady, nonlinear groundwater flow through porous media, *J. Coastal Res.* 50 (2007) 292–295.
- [40] A. Molabahrami, F. Khani, The homotopy analysis method to solve the Burgers–Huxley equation, *Nonlinear Anal. B Real World Appl.* (2007), doi:10.1016/j.nonrwa.2007.10.014, in press.
- [41] A.S. Bataineh, M.S.M. Noorani, I. Hashim, Solutions of time-dependent Emden–Fowler type equations by homotopy analysis method, *Phys. Lett. A* 371 (2007) 72–82.
- [42] Z. Wang, L. Zou, H. Zhang, Applying homotopy analysis method for solving differential–difference equation, *Phys. Lett. A* 369 (2007) 77–84.
- [43] Mustafa Inc., On exact solution of Laplace equation with Dirichlet and Neumann boundary conditions by the homotopy analysis method, *Phys. Lett. A* 365 (2007) 412–415.

- [44] W.H. Cai, Nonlinear dynamics of thermal-hydraulic networks, PhD thesis, University of Notre Dame, 2006.
- [45] Y. Song, L.C. Zheng, X.X. Zhang, On the homotopy analysis method for solving the boundary layer flow problem over a stretching surface with suction and injection, *J. Univ. Sci. Technol. Beijing* 28 (2006) 782–784 (in Chinese).
- [46] S.J. Liao, E. Magyari, Exponentially decaying boundary layers as limiting cases of families of algebraically decaying ones, *Z. Angew. Math. Phys.* 57 (5) (2006) 777–792.
- [47] S.J. Liao, A new branch of solutions of boundary-layer flows over a permeable stretching plate, *Internat. J. Non-Linear Mech.* 42 (2007) 819–830.